

# Analyses of axisymmetric waves in layered piezoelectric rods and their composites

Adnan H. Nayfeh,<sup>a)</sup> Wael G. Abdelrahman,<sup>b)</sup> and Peter B. Nagy<sup>c)</sup>

*Department of Aerospace Engineering and Engineering Mechanics, University of Cincinnati, Cincinnati, Ohio 45221-0070*

(Received 25 November 1999; accepted for publication 22 June 2000)

An exact treatment of the propagation of axisymmetric waves in coaxial anisotropic assembly of piezoelectric rod systems is presented. The rod system consists of an arbitrary number of coaxial layers, each possessing transversely isotropic symmetry properties. The treatment, which is based on the transfer matrix technique, is capable of deriving the dispersion relations for a variety of situations. These include the case of a single rod system that is either embedded in an infinitely extended solid or fluid host or kept free. The procedure is also adapted to derive approximate solutions for the cases of a periodic fiber distribution in a matrix material, which model unidirectional fiber-reinforced composites. The results are numerically illustrated for a widely used piezoelectric-polymer composite. It is seen that piezoelectric coupling can significantly change the morphology of the dispersive behavior of the composite. © 2000 Acoustical Society of America. [S0001-4966(00)02410-3]

PACS numbers: 43.25.Cg [HEB]

## I. INTRODUCTION

In a recent paper,<sup>1</sup> Nayfeh and Nagy presented a unified study of the propagation of axisymmetric longitudinal waves in coaxial anisotropic elastic fibers with application to a variety of their composites. The fiber bundle system consisted of an arbitrary number of coaxial layers, each possessing transverse isotropic symmetry and bonded at their interfaces in accordance with specified fashions. In the form of applications, the bundle was either embedded in an infinitely extended elastic solid or fluid host or kept free. Uniformly distributed bundles in a matrix material which model unidirectional bundle fiber-reinforced composites were also studied.

The solutions in Ref. 1 were obtained using the matrix transfer technique, originally introduced by Thomson<sup>2</sup> and later on enhanced by Haskell,<sup>3</sup> both for the study of wave interaction with layered isotropic flat media. Recently, this technique has been extensively used by a large number of investigators in a variety of wave propagation applications in layered media, often including cases of anisotropy. Most of this recent literature deals with flat layers. It is not the intent of the present work to review this vast literature. However, for the interested reader on this subject, we refer to Nayfeh.<sup>4</sup>

Up to quite recently, much fewer applications of the matrix transfer method to cylindrical layered media have been reported. In its application to the cylindrical systems of Ref. 1, the specific steps taken in constructing the model are summarized as follows: formal solutions in terms of Bessel functions are first obtained for each layer in terms of its displacement amplitudes. By specializing these solutions to the outer and inner faces (radii) of the layer, followed by eliminating the common displacement amplitudes, the local

transfer matrix for the layer is constructed. This matrix relates the field variables (the displacements and stress components) of one face of the layer to its other one. Such a matrix relation can be used, in conjunction with satisfying appropriate interface conditions across neighboring layers, to directly relate the field variables at the inner face of one layer to the outer face of its outer neighbor. When this procedure is carried out consecutively for all layers in the bundle, a global transfer matrix, the product of the individual transfer matrices, results, which relates the field variables at the outer face of the bundle to those at its inner face or vice versa.

The global matrix is then used for all of the specific applications outlined above. For cases involving infinite solid or fluid hosts, the formal solution for the host has to be specialized to insure satisfying the radiation conditions far away from the bundle–host interface; this requires the field variables to stay bounded deep in the host. If the inner component of the bundle is solid with no concentric hole, its local transfer matrix has to be adjusted such that its field variables will not encounter the usual singularities. Finally, in simulating the bundle fiber-reinforced composite, the repeating hexagonal unit cell of the composite is isolated, approximated by a concentric cylindrical system and, due to its inherent symmetry, the vanishing of the radial displacement and shear stress components are imposed on its outer boundary.

The aim of the present article is to extend the results of Ref. 1 and present a parallel treatment for rod-bundle systems including piezoelectric effects. This problem has diverse applications in fields such as medical composite transducer design, fiber optics, signal processing, and nondestructive testing. Up to quite recently, it was believed that cylindrical geometry, together with piezoelectric coupling (which is inherently anisotropic), lead to algebraic complications in the attempt of obtaining exact solutions. That is perhaps why exact treatments of problems dealing

<sup>a)</sup>Electronic mail: anayfeh@uceng.uc.edu

<sup>b)</sup>Electronic mail: abdelrw1@email.uc.edu

<sup>c)</sup>Electronic mail: pnagy@uceng.uc.edu

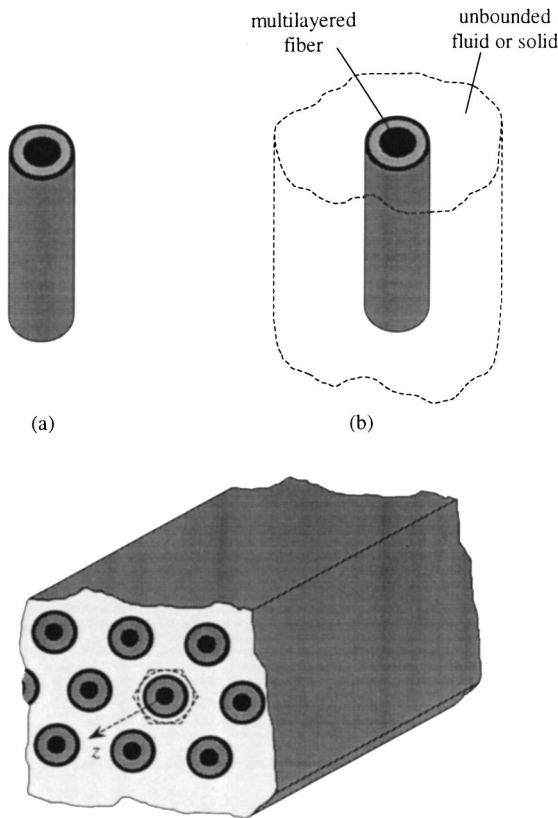


FIG. 1. Schematic diagram of (a) a single free multilayered rod, (b) a single multilayered rod embedded in a solid host or immersed in a fluid, and (c) an infinite unidirectional fibrous reinforced composite with periodically distributed multilayered fibers.

with piezoelectric rods are relatively rare. Nevertheless, our literature search revealed some limited, but relevant, publications that deal with exact analyses of piezoelectric rods.<sup>5,6</sup> Reference 5 treats vibrations of circular cylindrical shells and Ref. 6 develops exact solutions for waves in a single infinitely clad rod. For the interested reader, there is, however, a relatively larger body of literature that exists for the treatment of wave interaction with flat layered piezoelectric systems. Once again, while it is not the intent of the present work to give a complete account of this literature, we draw attention to some recent samples.<sup>4,7-10</sup>

## II. FORMULATION OF THE PROBLEM

### A. Field equations

Consider the multilayered rod systems of Fig. 1. Schematic 1(a) represents a single free multilayered rod, whereas Fig. 1(b) shows the case of a single multilayered rod embedded in an unbounded solid host or immersed in an unbounded fluid. Figure 1(c) shows the case of a periodic distribution of multilayered fibers in a fibrous-reinforced composite. Each of the rods of Fig. 1 consists of an arbitrary number  $p$  of transversely isotropic layers rigidly bonded at their interfaces and lined up such that their axes of symmetry coincide with each other and also with the reference coordinate axis  $z$ . The layers are consequently numbered  $1, 2, \dots, p$  from the host solid as shown in Fig. 2. In our subsequent

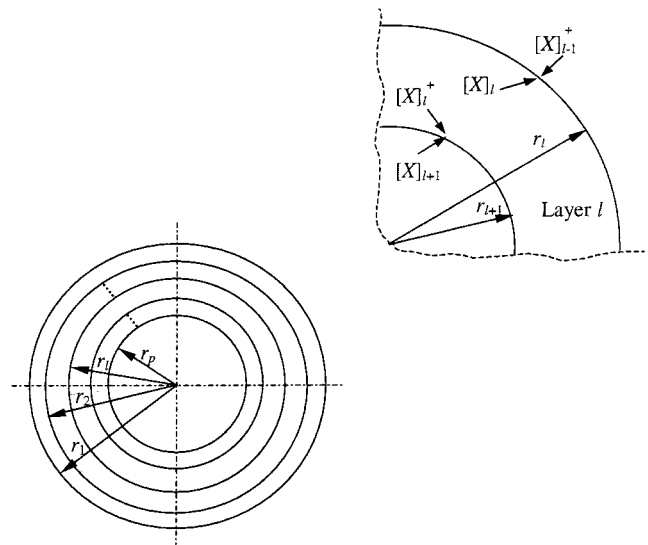


FIG. 2. Geometry of the multilayered system.

discussions, we reserve the subscripts “ $h$ ” and “ $f$ ” to designate the solid host material and fluid, respectively.

The outer surface of a typical layer  $l$  is located at the location  $r = r_l$  measured from the center of the cylinder. It follows that the thickness of layer  $l$  will be  $r_l - r_{l+1}$  and hence the total radius of the cylinder will be  $r_1$ , i.e., the distance to the location of the host-rod interface.

With these restrictions on the geometry and the propagation directions for longitudinal waves, the motion is reduced to an axisymmetric one. Here, the displacement component  $u_\theta$  vanishes and the remaining field variables are independent of  $\theta$ . The relevant piezoelectric field equations which hold for each layer and also for the solid host consist of the following:

(i) the momentum equations

$$\frac{\partial \sigma_r}{\partial r} + \frac{\partial \sigma_{rz}}{\partial z} + \frac{1}{r}(\sigma_r - \sigma_\theta) = \rho \frac{\partial^2 u_r}{\partial t^2}, \quad (1a)$$

$$\frac{\partial \sigma_z}{\partial z} + \frac{1}{r} \frac{\partial}{\partial r}(r \sigma_{rz}) = \rho \frac{\partial^2 u_z}{\partial t^2}, \quad (1b)$$

and the charge equation of electrostatics

$$\frac{\partial D_z}{\partial z} + \frac{1}{r} \frac{\partial}{\partial r}(r D_r) = 0; \quad (2)$$

(ii) the coupled constitutive relations

$$\sigma_{ij} = c_{ijkl}^E S_{kl} - e_{kij} E_k, \quad (3a)$$

$$D_i = e_{ikl} S_{kl} + \epsilon_{ik}^S E_k; \quad (3b)$$

(iii) the strain-mechanical displacement relations

$$S_r = \frac{\partial u_r}{\partial r}, \quad S_\theta = \frac{u_r}{r}, \quad (4)$$

$$S_z = \frac{\partial u_z}{\partial z}, \quad S_{rz} = \frac{1}{2} \left( \frac{\partial u_z}{\partial r} + \frac{\partial u_r}{\partial z} \right),$$

and the electric field-electric potential relations

$$E_r = -\frac{\partial \phi}{\partial r}, \quad E_z = -\frac{\partial \phi}{\partial z}. \quad (5)$$

In our subsequent analysis, we shall allow the subscripts  $r, \theta, z$  to be synonymous with 1, 2, 3, respectively. We also recognize that  $\sigma_r, \sigma_z, S_r,$  and  $S_z$  are conveniently constructed and stand for  $\sigma_{rr}, \sigma_{zz}, S_{rr},$  and  $S_{zz},$  respectively. In Eqs. (1)–(5) we then have  $i, j, k, l = 1, 2, 3;$   $\sigma_{ij}, u_i, D_i, S_{ij}, E_i$  are the components of stress, mechanical displacement, electric displacement, mechanical strain, and electric field, respectively;  $\rho$  and  $\phi$  are the mass density and the electric potential;  $c_{ijkl}^E$  are the elastic moduli for a constant electric field;  $\epsilon_{ik}^S$  are the dielectric coefficients for a constant strain field, and  $e_{kij}$  are the piezoelectric constants.

The elastic, piezoelectric, and dielectric constants for the transversely isotropic piezoelectric system are given in the expanded matrix forms

$$C_{pq}^E = \begin{bmatrix} C_{11}^E & C_{12}^E & C_{13}^E & 0 & 0 & 0 \\ C_{12}^E & C_{11}^E & C_{13}^E & 0 & 0 & 0 \\ C_{13}^E & C_{13}^E & C_{33}^E & 0 & 0 & 0 \\ 0 & 0 & 0 & C_{44}^E & 0 & 0 \\ 0 & 0 & 0 & 0 & C_{44}^E & 0 \\ 0 & 0 & 0 & 0 & 0 & C_{66}^E \end{bmatrix}, \quad (6)$$

where

$$2C_{66}^E = (C_{11}^E - C_{12}^E),$$

$$e_{ip} = \begin{bmatrix} 0 & 0 & 0 & 0 & e_{15} \\ 0 & 0 & 0 & e_{15} & 0 \\ e_{31} & e_{31} & e_{33} & 0 & 0 \end{bmatrix}, \quad (7)$$

$$\epsilon_{ij}^S = \begin{bmatrix} \epsilon_{11}^S & 0 & 0 \\ 0 & \epsilon_{11}^S & 0 \\ 0 & 0 & \epsilon_{33}^S \end{bmatrix}, \quad (8)$$

which reflects the usual renaming of  $c_{ijkl}, i, j, k, l = 1, 2, 3,$  as  $C_{pq}, p, q = 1, 2, \dots, 6.$  For simplicity of notation, we shall thereafter suppress the superscripts  $E$  and  $S$  in the equations (6) and (8). According to the above relations, the constitutive equations (3) take the expanded forms

$$\sigma_r = C_{11} \frac{\partial u_r}{\partial r} + C_{12} \frac{u_r}{r} + C_{13} \frac{\partial u_z}{\partial z} + e_{31} \frac{\partial \phi}{\partial z}, \quad (9a)$$

$$\sigma_z = C_{13} \frac{1}{r} \frac{\partial}{\partial r} (ru_r) + C_{33} \frac{\partial u_z}{\partial z} + e_{33} \frac{\partial \phi}{\partial z}, \quad (9b)$$

$$\sigma_{rz} = C_{44} \left( \frac{\partial u_z}{\partial r} + \frac{\partial u_r}{\partial z} \right) + e_{15} \frac{\partial \phi}{\partial r}, \quad (9c)$$

$$D_r = \frac{e_{15}}{2} \left( \frac{\partial u_z}{\partial r} + \frac{\partial u_r}{\partial z} \right) - \epsilon_{11} \frac{\partial \phi}{\partial r}. \quad (9d)$$

$$D_z = e_{31} \frac{1}{r} \frac{\partial}{\partial r} (ru_r) + e_{33} \frac{\partial u_z}{\partial z} - \epsilon_{33} \frac{\partial \phi}{\partial z}, \quad (9e)$$

which, once again, hold for all layers.

## B. Solution of the equations

Details of the procedure used here are readily available in Ref. 1. For the present system, the field equations (1) and (2) are combined with the constitutive relations (9) to yield the three coupled equations

$$C_{11} \frac{\partial^2 u_r}{\partial r^2} + \frac{C_{11}}{r} \left( \frac{\partial u_r}{\partial r} - \frac{u_r}{r} \right) + C_{44} \frac{\partial^2 u_r}{\partial z^2} + (C_{13} + C_{44}) \frac{\partial^2 u_z}{\partial r \partial z} + (e_{31} + e_{15}) \frac{\partial^2 \phi}{\partial r \partial z} = \rho \frac{\partial^2 u_r}{\partial t^2},$$

$$C_{33} \frac{\partial^2 u_z}{\partial z^2} + C_{44} \left( \frac{\partial^2 u_z}{\partial r^2} + \frac{1}{r} \frac{\partial u_z}{\partial r} \right) + (C_{13} + C_{44}) \times \left( \frac{\partial^2 u_r}{\partial r \partial z} + \frac{1}{r} \frac{\partial u_r}{\partial z} \right) + e_{33} \frac{\partial^2 \phi}{\partial z^2} + e_{15} \left( \frac{\partial^2 \phi}{\partial r^2} + \frac{1}{r} \frac{\partial \phi}{\partial r} \right) = \rho \frac{\partial^2 u_z}{\partial t^2}, \quad (10)$$

$$(e_{31} + e_{15}) \left( \frac{\partial^2 u_r}{\partial r \partial z} + \frac{1}{r} \frac{\partial u_r}{\partial z} \right) + e_{33} \frac{\partial^2 u_z}{\partial z^2} + e_{15} \left( \frac{\partial^2 u_z}{\partial r^2} + \frac{1}{r} \frac{\partial u_z}{\partial r} \right) - \epsilon_{33} \frac{\partial^2 \phi}{\partial z^2} - \epsilon_{11} \left( \frac{\partial^2 \phi}{\partial r^2} + \frac{1}{r} \frac{\partial \phi}{\partial r} \right) = 0.$$

For a wave propagating along the  $z$  direction, the formal solution for  $u_r, u_z,$  and  $\phi$  are given, parallel to the analysis in Ref. 1, as

$$(u_r, u_z, \phi) = [U_1 \beta_1(\gamma r), U_2 \beta_0(\gamma r), U_3 \beta_0(\gamma r)] e^{i(kz - \omega t)}, \quad (11)$$

where  $\gamma$  is an unknown parameter,  $k$  is the longitudinal wave number related to the frequency and phase velocity as  $k = \omega/c,$  and  $\beta_0$  and  $\beta_1$  are zeroth- and first-order Bessel functions of the first or the second kind.

Substituting this solution into Eqs. (10) yields a set of three linear homogeneous equations in the amplitudes. In matrix form, these are

$$\begin{bmatrix} \rho \omega^2 - C_{11} \gamma^2 - C_{44} k^2 & -ik \gamma (C_{13} + C_{44}) & -ik \gamma (e_{31} + e_{15}) \\ ik \gamma (C_{13} + C_{44}) & \rho \omega^2 - C_{33} k^2 - C_{44} \gamma^2 & -(e_{33} k^2 + e_{15} \gamma^2) \\ ik \gamma (e_{31} + e_{15}) & -(e_{33} k^2 + e_{15} \gamma^2) & \epsilon_{33} k^2 + \epsilon_{11} \gamma^2 \end{bmatrix} \begin{Bmatrix} U_1 \\ U_2 \\ U_3 \end{Bmatrix} = \underline{0}. \quad (12)$$

For nonzero solution of the amplitudes, the determinant of this equation must vanish. This yields a sixth-order polynomial in  $\gamma$  (cubic in  $\gamma^2$ ), relating it to the radial frequency  $\omega$ . It admits six solutions which we number as  $\gamma_1(\omega, k)$ ,

$\gamma_2(\omega, k)$ ,  $\gamma_3(\omega, k)$ ,  $\gamma_4(\omega, k)$ ,  $\gamma_5(\omega, k)$ , and  $\gamma_6(\omega, k)$ , where  $\gamma_4 = -\gamma_1$ ,  $\gamma_5 = -\gamma_2$ , and  $\gamma_6 = -\gamma_3$ . For each  $\gamma_q$ ,  $q = 1, 2, \dots, 6$ , Eq. (12) yields the amplitude ratios  $V_q = U_{2q}/U_{1q}$  and  $W_q = U_{3q}/U_{1q}$ ,  $q = 1, 2, \dots, 6$ , as

$$V_q = \frac{k^2 \gamma_q^2 (C_{13} + C_{44})(e_{31} + e_{15}) + (\rho \omega^2 - C_{11} \gamma_q^2 - C_{44} k^2)(e_{33} k^2 + e_{15} \gamma_q^2)}{ik \gamma_q [(C_{13} + C_{44})(e_{33} k^2 + e_{15} \gamma_q^2) + (\rho \omega^2 - C_{33} k^2 - C_{44} \gamma_q^2)(e_{31} + e_{15})]},$$

$$W_q = \frac{(\rho \omega^2 - C_{11} \gamma_q^2 - C_{44} k^2)(\rho \omega^2 - C_{33} k^2 - C_{44} \gamma_q^2) - k^2 \gamma_q^2 (C_{13} + C_{44})^2}{ik \gamma_q [(C_{13} + C_{44})(e_{33} k^2 + e_{15} \gamma_q^2) + (\rho \omega^2 - C_{33} k^2 - C_{44} \gamma_q^2)(e_{31} + e_{15})]}.$$
(13a)

Inspecting Eq. (13a) reveals the interesting and important relations

$$V_4 = -V_1, \quad V_5 = -V_2, \quad V_6 = -V_3.$$
(13b)

The same relations also hold for  $W_q$ .

Using the principle of superposition, together with the constitutive relations (9), the formal solution for the relevant displacements, stresses, electric potential, and electric displacement in each layer  $l$  are combinations of Bessel functions of the first and second kind. These formal solutions can be written in the expanded matrix form

$$\begin{Bmatrix} u_r \\ u_z \\ \phi \\ \sigma_r \\ \sigma_{rz} \\ D_r \end{Bmatrix}_l = \begin{bmatrix} J_1(\gamma_1 r) & Y_1(\gamma_1 r) & J_1(\gamma_2 r) & Y_1(\gamma_2 r) & J_1(\gamma_3 r) & Y_1(\gamma_3 r) \\ V_1 J_0(\gamma_1 r) & V_1 Y_0(\gamma_1 r) & V_2 J_0(\gamma_2 r) & V_2 Y_0(\gamma_2 r) & V_3 J_0(\gamma_3 r) & V_3 Y_0(\gamma_3 r) \\ W_1 J_0(\gamma_1 r) & W_1 Y_0(\gamma_1 r) & W_2 J_0(\gamma_2 r) & W_2 Y_0(\gamma_2 r) & W_3 J_0(\gamma_3 r) & W_3 Y_0(\gamma_3 r) \\ D_{11} & \bar{D}_{11} & D_{12} & \bar{D}_{12} & D_{13} & \bar{D}_{13} \\ D_{21} & \bar{D}_{21} & D_{22} & \bar{D}_{22} & D_{23} & \bar{D}_{23} \\ D_{31} & \bar{D}_{31} & D_{32} & \bar{D}_{32} & D_{33} & \bar{D}_{33} \end{bmatrix}_l \begin{Bmatrix} A_1 \\ \bar{A}_1 \\ A_2 \\ \bar{A}_2 \\ A_3 \\ \bar{A}_3 \end{Bmatrix}_l,$$
(14)

where

$$D_{1q} = (C_{11} \gamma_q + ik C_{13} V_q + ik e_{31} W_q) J_0(\gamma_q r) - (C_{11} - C_{12}) \frac{J_1(\gamma_q r)}{r},$$

$$\bar{D}_{1q} = (C_{11} \gamma_q + ik C_{13} V_q + ik e_{31} W_q) Y_0(\gamma_q r) - (C_{11} - C_{12}) \frac{Y_1(\gamma_q r)}{r},$$

$$D_{2q} = (ik C_{44} - C_{44} V_q \gamma_q - e_{15} W_q \gamma_q) J_1(\gamma_q r),$$

$$\bar{D}_{2q} = (ik C_{44} - C_{44} V_q \gamma_q - e_{15} W_q \gamma_q) Y_1(\gamma_q r),$$

$$D_{3q} = (ik e_{15} - e_{15} V_q \gamma_q + \varepsilon_{11} W_q \gamma_q) J_1(\gamma_q r),$$

$$\bar{D}_{3q} = (ik e_{15} - e_{15} V_q \gamma_q + \varepsilon_{11} W_q \gamma_q) Y_1(\gamma_q r).$$
(15)

To facilitate our subsequent analysis, this equation is rewritten in the compact form

$$U_l = X_l A_l,$$
(16)

where  $U_l$  is the column matrix of the field variable components,  $X_l$  is the  $6 \times 6$  square matrix in Eq. (14), and  $A_l$  is the column matrix of the wave amplitudes. This equation is supplemented with the continuity conditions

$$\begin{Bmatrix} u_r \\ u_z \\ \phi \\ \sigma_r \\ \sigma_{rz} \\ D_r \end{Bmatrix}_l = \begin{Bmatrix} u_r \\ u_z \\ \phi \\ \sigma_r \\ \sigma_{rz} \\ D_r \end{Bmatrix}_{l+1} \quad \text{at } r = r_{l+1}.$$
(17)

### C. Local transfer matrix

Equation (14) can be specialized to the inner and outer radii  $r = r_{l+1}$  and  $r = r_l$  of layer  $l$ , respectively, as

$$U_l^- = X_l^- A_l \quad \text{at } r = r_l,$$
(18)

$$U_l^+ = X_l^+ A_l \quad \text{at } r = r_{l+1}.$$
(19)

Eliminating the common amplitude vector  $A_l$ , we relate  $U_l^-$  to  $U_l^+$  as

$$U_l^- = M_l U_l^+,$$
(20)

where

$$M_l = X_l^- (X_l^+)^{-1}$$
(21)

is the  $6 \times 6$  local individual transfer matrix for layer  $l$ , which relates the displacements, stresses, electric potential, and electric displacement at its outer surface to those at the inner surface. The superscripts  $\pm$  are used here to label the inner and outer boundaries, respectively.

## D. Global transfer matrix

By invoking the continuity conditions (17), we relate the stresses, displacements, electric potential, and electric displacement at the outer radius of the total system,  $r=r_1$ , to those at the inner radius,  $r=r_p$ , via the global transfer matrix  $M$  as

$$U_1^- = MU_{p-1}^+, \quad (22)$$

where

$$M = M_1 M_2 \cdots M_{p-1}. \quad (23)$$

Invoking the continuity at the interface between layer  $p-1$  and the core  $p$  leads to

$$U_{p-1}^+ = U_p^-. \quad (24)$$

According to Eq. (18), for the core material we have

$$U_p^- = X_p^- A_p. \quad (25)$$

Then Eq. (22) takes the form

$$U_1^- = QA_p, \quad (26)$$

where

$$Q = MX_p^-. \quad (27)$$

To avoid singularities at the origin in the core, the amplitudes  $\bar{A}_1, \bar{A}_2, \bar{A}_3$  should vanish, leading to

$$\begin{Bmatrix} u_r \\ u_z \\ \phi \\ \sigma_{rr} \\ \sigma_{rz} \\ D_r \end{Bmatrix}_l = \begin{bmatrix} Q_{11} & Q_{12} & Q_{13} & Q_{14} & Q_{15} & Q_{16} \\ Q_{21} & Q_{22} & Q_{23} & Q_{24} & Q_{25} & Q_{26} \\ Q_{31} & Q_{32} & Q_{33} & Q_{34} & Q_{35} & Q_{36} \\ Q_{41} & Q_{42} & Q_{43} & Q_{44} & Q_{45} & Q_{46} \\ Q_{51} & Q_{52} & Q_{53} & Q_{54} & Q_{55} & Q_{56} \\ Q_{61} & Q_{62} & Q_{63} & Q_{64} & Q_{65} & Q_{66} \end{bmatrix}_{sys} \begin{Bmatrix} A_1 \\ 0 \\ A_2 \\ 0 \\ A_3 \\ 0 \end{Bmatrix}_p. \quad (28)$$

For the interested reader, some interesting properties of both the local and global transfer matrices are listed in Ref. 1.

## III. APPLICATIONS

### A. Free multilayered rod system

We start by deriving the dispersion relation for cases involving free rods. A “free” rod is meant to be mechanically free, i.e., both normal  $\sigma_r$  and tangential  $\sigma_{rz}$  stresses must vanish at the surface, but it is still immersed in a dielectric medium, namely vacuum. Theoretically, the guided modes of a free piezoelectric rod become leaky at the cutoff frequencies where the phase velocity becomes infinitely

high. However, the electromagnetic wavelength is so high relative to the acoustic one that electromagnetic radiation cannot occur except at these singularities and the modes are true guided waves with real wave numbers. Of course the velocity of the guided modes still could be perceivably affected by the pure imaginary electromagnetic radiation load of the surrounding vacuum, but the relative permittivity of the piezoelectric material is typically so high that the normal component of the dielectric displacement  $D_r$  can be also assumed to vanish at the “free” surface, which significantly simplifies the calculations. If we identify the rod outer radius  $r_1$  with  $a$ , and invoke the free boundary conditions, namely  $\sigma_r = \sigma_{rz} = D_r = 0$  at  $r = a$ , then Eq. (28) reduces to the characteristic equation

$$\begin{vmatrix} Q_{41} & Q_{43} & Q_{45} \\ Q_{51} & Q_{53} & Q_{55} \\ Q_{61} & Q_{63} & Q_{65} \end{vmatrix}_p = 0, \quad (29)$$

relating phase velocity  $c$  to the wave number  $k$ .

### B. Multilayered rod system embedded in a solid host

For cases involving a multilayered rod embedded in an infinitely extended solid host, it was shown in Ref. 1 that formal solutions in the host material are expressed in terms of Hankel functions of the first kind, namely,

$$H_n = J_n + iY_n, \quad (30)$$

since only outgoing waves are allowed physically in an unbounded medium. The formal solutions for the field variables in the host take the form

$$\begin{aligned} u_{rh} &= A_1 H_1(\gamma_{1h}a) + A_2 H_1(\gamma_{2h}a) + A_3 H_1(\gamma_{3h}a), \\ u_{zh} &= A_1 V_{1h} H_1(\gamma_{1h}a) + A_2 V_{2h} H_1(\gamma_{2h}a) \\ &\quad + A_3 V_{3h} H_1(\gamma_{3h}a), \\ \phi_h &= A_1 W_{1h} H_1(\gamma_{1h}a) + A_2 W_{2h} H_1(\gamma_{2h}a) \\ &\quad + A_3 W_{3h} H_1(\gamma_{3h}a), \end{aligned} \quad (31)$$

where a subscript  $h$  means “specialized to the host material.” The rest of the field variables  $\sigma_r, \sigma_{rz}$ , and  $D_r$  are calculated from Eqs. (9a), (9c), and (9d), when specialized for the host material. Applying the continuity conditions at the host–rod interface, namely

$$\begin{Bmatrix} u_r \\ u_z \\ \phi \\ \sigma_r \\ \sigma_{rz} \\ D_r \end{Bmatrix}_0 = \begin{Bmatrix} u_r \\ u_z \\ \phi \\ \sigma_r \\ \sigma_{rz} \\ D_r \end{Bmatrix}_1^- \quad \text{at } r=r_1=a, \quad (32)$$

yields the characteristic equation

$$\begin{vmatrix} Q_{11} & Q_{13} & Q_{15} & -H_1(\gamma_{1h}a) & -H_1(\gamma_{2h}a) & -H_1(\gamma_{3h}a) \\ Q_{21} & Q_{23} & Q_{25} & -V_{1h}H_0(\gamma_{1h}a) & -V_{2h}H_0(\gamma_{2h}a) & -V_{3h}H_0(\gamma_{3h}a) \\ Q_{31} & Q_{33} & Q_{35} & -W_{1h}H_0(\gamma_{1h}a) & -W_{2h}H_0(\gamma_{2h}a) & -W_{3h}H_0(\gamma_{3h}a) \\ Q_{41} & Q_{43} & Q_{45} & -D_{11h} & -D_{12h} & -D_{13h} \\ Q_{51} & Q_{53} & Q_{55} & -D_{21h} & -D_{22h} & -D_{23h} \\ Q_{61} & Q_{63} & Q_{65} & -D_{31h} & -D_{32h} & -D_{33h} \end{vmatrix} = 0, \quad (33)$$

where

$$\begin{aligned} D_{1qh} &= (C_{11}\gamma_{qh} + ikC_{13}V_{qh} + ike_{31}W_{qh})H_0(\gamma_{qh}r) \\ &\quad - (C_{11} - C_{12}) \frac{H_1(\gamma_{qh}r)}{r}, \\ D_{2qh} &= (ikC_{44} - C_{44}V_{qh}\gamma_{qh} - e_{15}W_{qh}\gamma_{qh})H_1(\gamma_{qh}r), \\ D_{3qh} &= (ike_{15} - e_{15}V_{qh}\gamma_{qh} + \varepsilon_{11}W_{qh}\gamma_{qh})H_1(\gamma_{qh}r). \end{aligned}$$

### C. Multilayered rod system immersed in fluid

The formal solutions in an unbounded fluid host can be obtained directly from those of a solid host, noting that no shear deformations exist in fluids. These solutions are

$$\begin{aligned} u_{rf} &= CH_1(\gamma_f r), \\ u_{zf} &= -(ik/\gamma_f)CH_1(\gamma_f r), \\ \sigma_{rf} &= (\rho_f \omega^2 / \gamma_f)CH_0(\gamma_f r), \end{aligned} \quad (34)$$

where the radial wave number in the fluid  $\gamma_f$  is calculated for the isotropic fluid from

$$\gamma_f^2 = \omega^2 / c_f^2 - k^2, \quad (35)$$

and where  $c_f$  is the sound velocity in the fluid. As in the case of free rods, a similar problem arises for rods immersed in a dielectric fluid. The relatively high permittivity of polar fluids like water ( $\varepsilon \approx 80\varepsilon_0$ ) could possibly affect the electrical boundary conditions so much that the guided mode velocities change perceptibly. This effect will be further investigated in a separate paper and in the following we will assume that the normal component of the dielectric displacement  $D_r$  vanishes at the surface of an immersed rod.

Satisfying the interface conditions between the fluid and the rod, namely  $u_r^- = u_{rf}$ ,  $\sigma_r^- = \sigma_{rf}$ ,  $\sigma_{rz}^- = 0$ , and  $D_r^- = 0$  at  $r = r_1 = a$ , leads to the required characteristic equation

$$\begin{vmatrix} Q_{11} & Q_{13} & Q_{15} & -H_1(\gamma_f a) \\ Q_{41} & Q_{43} & Q_{45} & -(\rho_f \omega^2 / \gamma_f)H_0(\gamma_f a) \\ Q_{51} & Q_{53} & Q_{55} & 0 \\ Q_{61} & Q_{63} & Q_{65} & 0 \end{vmatrix} = 0. \quad (36)$$

### D. Periodic fibrous systems

For the case of infinitely extended medium consisting of a periodic array of unidirectional fibrous composites [see Fig. 1(c)], the symmetry of the problem allows isolating the repeating hexagonal cell and approximating it by a concentric cylindrical layered fiber surrounded by a coaxial matrix

layer. With regard to Fig. 2, this matrix layer is called layer 1, and the fiber layers are layers 2, 3, ...,  $p$ . As pointed out in Ref. 1, the inherent periodicity and symmetry of the unbounded composite imply the vanishing of the lateral displacement  $u_r$ , the shear stress  $\sigma_{rz}$ , and the lateral electric displacement  $D_r$  at the outer radius of the fiber-matrix system. These boundary conditions should be contrasted with those appropriate for the free and clad systems where stress-free conditions are invoked at the outer boundaries. Furthermore, we recognize that the hexagonal-cylinder approximations do not accurately account for the structural details of the composite. At low frequencies, the error caused by this approximation can be essentially eliminated by adjusting the diameter of the matrix cladding so that the fiber volume fraction is accurately represented. In this case, the distance between neighboring fibers in the real hexagonal composite is slightly less than the diameter chosen for the clad fiber in the cylindrical model. For example, in the case of 25% fiber volume fraction, the distance between neighboring fibers in the real hexagonal composite is only  $\approx 1.905$  times the fiber diameter while the outer diameter of the clad fiber in the cylindrical model is exactly twice the fiber diameter. At high frequencies, when the acoustic wavelength becomes smaller than the fiber diameter, some error will inevitably arise as the wave velocity becomes more and more sensitive to the matrix geometry, too, rather than just the relative amount of matrix material in the composite. The shape difference between the approximate and real matrix geometry becomes more significant at high fiber volume fractions, therefore it is expected that the approximation breaks down above approximately 50% reinforcement. Although exact solutions are currently not available for comparison, it is clear that the above-described cylindrical model is more accurate at relatively low fiber volume fractions and at low normalized frequencies.

In the cylindrical approximation of infinite media, Eq. (29) can be translated into the following characteristic dispersion equation:

$$\begin{vmatrix} Q_{11} & Q_{13} & Q_{15} \\ Q_{51} & Q_{53} & Q_{55} \\ Q_{61} & Q_{63} & Q_{65} \end{vmatrix}_p = 0. \quad (37)$$

## IV. NUMERICAL RESULTS

The material properties used in the following calculations are listed in Table I. In addition, we can introduce effective coupling coefficients to quantify the strength of pi-

TABLE I. The dimensions and material properties of illustration materials. Units of  $C_{pq}$  and  $e_{ip}$  are  $10^9$  N/m<sup>2</sup> and Co/m<sup>2</sup>, respectively.  $\epsilon_{ij}$  is given nondimensional as  $\epsilon^j/\epsilon_0^j$ , where  $\epsilon_0^j = 8.854 \times 10^{-12}$  F/m.

Material	PZT 65/35	Spurr
Radius (mm)	0.707	1.0
$\rho$ (g/cm <sup>3</sup> )	7.500	1.100
$C_{11}$	159.4	5.3
$C_{12}$	73.9	3.1
$C_{13}$	73.9	3.1
$C_{22}$	159.4	5.3
$C_{23}$	73.9	3.1
$C_{33}$	126.1	5.3
$C_{44}$	38.9	1.1
$C_{55}$	38.9	1.1
$C_{66}$	42.8	1.1
$e_{33}$	10.7	0
$e_{32}$	-6.13	0
$e_{31}$	-6.13	0
$e_{15}$	8.39	0
$e_{24}$	8.39	0
$\epsilon_{11}$	639.3	1
$\epsilon_{22}$	639.3	1
$\epsilon_{33}$	153.3	1

ezelectric coupling in different situations. In the following, we are going to use an asterisk to indicate effective parameters of the piezoelectric material. For example, in the plane of isotropy of an infinite transversely isotropic material (radial direction), only the vertically polarized shear wave velocity,  $c_{s1}^* = \sqrt{C_{44}^*/\rho} = \sqrt{C_{44}(1 + \kappa_1^2)/\rho} = c_{s1} \sqrt{1 + \kappa_1^2}$ , is affected by the piezoelectric coupling while the longitudinal velocity is not,  $c_{d1}^* = c_{d1} = \sqrt{C_{11}/\rho}$ . In contrast, normal to the plane of isotropy (axial direction), only the longitudinal wave velocity,  $c_{d2}^* = \sqrt{C_{33}^*/\rho} = \sqrt{C_{33}(1 + \kappa_2^2)/\rho} = c_{d2} \sqrt{1 + \kappa_2^2}$ , is affected by the piezoelectric coupling while the vertically polarized shear velocity is not,  $c_{s2}^* = c_{s2} = \sqrt{C_{44}/\rho}$ . These coupling coefficients can be calculated from  $\kappa_1^2 = e_{15}^2/(C_{44}\epsilon_{11})$  and  $\kappa_2^2 = e_{33}^2/(C_{33}\epsilon_{33})$  as  $\kappa_1 \approx 0.56$  and  $\kappa_2 \approx 0.82$  in the case of PZT 65/35.

Figure 3 shows the dispersion curves for the six lowest-order axisymmetric guided modes in a free transversely isotropic PZT 65/35 rod of  $a = 0.707$ -mm radius. The solid lines represent the actual piezoelectric material while the dashed lines represent a similar material with identical elastic constants and density but no piezoelectricity. The substantial overall difference between the two sets of dispersion curves clearly indicates the very strong effect of piezoelectric coupling on the axisymmetric modes. These differences can be summarized as follows. First, there is a surprisingly large drop in the phase velocity of the lowest-order mode at low frequencies. We calculated Young's modulus of a transversely isotropic piezoelectric rod in the axial direction from the static limit of the field equations as

$$E_3^* = C_{33} \frac{2C_{13}^2\epsilon_{33} + 4C_{13}e_{31}e_{33} - (C_{11} + C_{12})e_{33}^2}{(C_{11} + C_{12})\epsilon_{33} + 2e_{31}^2}. \quad (38)$$

In comparison, Young's modulus of a transversely isotropic nonpiezoelectric rod is

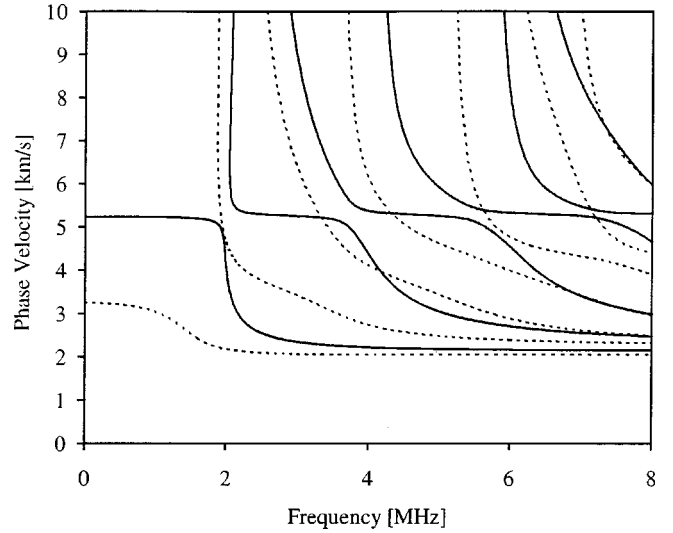


FIG. 3. Dispersion curves for the six lowest-order axisymmetric guided modes in a free transversely isotropic PZT 65/35 rod of  $a = 0.707$ -mm radius (solid lines—piezoelectric material, dashed lines—without piezoelectricity).

$$E_3 = C_{33} - 2C_{13}^2/(C_{11} + C_{12}). \quad (39)$$

We can write Young's modulus in terms of a characteristic coupling coefficient as  $E_3^* = E(1 + \kappa_E^2)$ , where  $\kappa_E \approx 1.26$  calculated for the PZT rod, indicating that it is larger than those of the bulk wave, i.e.,  $\kappa_1 < \kappa_2 < \kappa_E$ .

Second, there is also a significant upward shift in the cutoff frequencies of the higher-order modes. Generally, each mode is a combination of coupled quasi-shear and quasi-longitudinal waves. However, at the cutoff frequencies, the phase velocity becomes infinitely high and the partial waves propagate strictly in the plane of isotropy where they decouple into either pure shear or pure longitudinal modes. The shear-type (e.g., the first-order mode) cutoff frequencies can be simply calculated from

$$f_n^* = \frac{j_n c_{s1}^*}{2\pi a} = f_n \sqrt{1 + \kappa_1^2}, \quad (40)$$

where  $j_n$  is the  $n$ th zero of the first-order Bessel function of the first kind ( $J_1$ ). Accordingly, these cutoff frequencies are approximately 15% higher in a piezoelectric rod than in an otherwise identical but nonpiezoelectric one. Although it is not obvious from Fig. 3, which is limited to relatively low phase velocities, the longitudinal-type (e.g., the second-order mode) cutoff frequencies are not affected by piezoelectric coupling since the longitudinal mode propagating in the plane of isotropy is not affected, i.e.,  $c_{d1}^* = c_{d1} = \sqrt{C_{11}/\rho}$ . The longitudinal-type cutoff frequencies can be calculated from

$$f_m^* = \frac{g_m c_{d1}}{2\pi a} = f_m, \quad (41)$$

where  $g_m$  is the  $m$ th zero of the  $G(\xi) = J_1(\xi)/[\xi J_0(\xi)] - C_{11}/(C_{11} - C_{12})$  function.

Third, the strong piezoelectric coupling also manifests itself through the appearance of a relatively flat "plateau" region around 5200 m/s. All modes crossing this region ex-

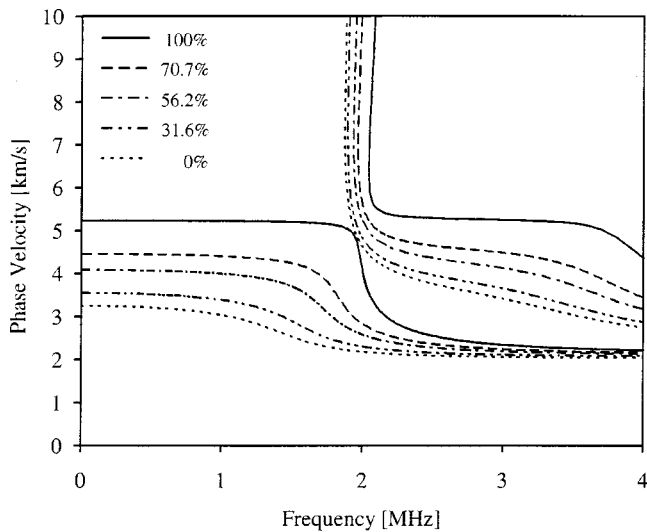


FIG. 4. Dispersion curves for the two lowest-order axisymmetric guided modes in a free transversely isotropic PZT 65/35 rod of  $a=0.707$ -mm radius with varying piezoelectric coupling. The piezoelectric coupling was decreased by proportionally increasing both  $\epsilon_{11}$  and  $\epsilon_{33}$  by the same amount with respect to their nominal values listed in Table I.

hibit an essentially flat dispersion curve over a fairly wide frequency range and these regions form a more or less continuous nondispersive branch.

The effect of piezoelectric coupling can be further investigated in more detail through the examples of the first two modes in the case of gradually increasing piezoelectric coupling. Figure 4 shows the dispersion curves for the two lowest-order axisymmetric guided modes in a free transversely isotropic PZT 65/35 rod of  $a=0.707$ -mm radius with varying piezoelectric coupling. The piezoelectric coupling was decreased by proportionally increasing both  $\epsilon_{11}$  and  $\epsilon_{33}$  by the same amount with respect to their nominal values listed in Table I. For example, a factor of 2 increase in the permittivities corresponds to 70.7% reduced piezoelectric coupling. Because of numerical difficulties, the nonpiezoelectric case was calculated by the numerical technique described in Ref. 1. These results well illustrate how the stiffening of the material caused by the gradual increase of the piezoelectric coupling modifies the dispersion curves by pushing them up towards higher phase velocities and to the right towards higher frequencies while the transitions between regions of low and high dispersion become sharper.

As an example of a multi-layered rod, Fig. 5 shows the dispersion curves for the six lowest-order axisymmetric guided modes in a transversely isotropic piezoelectric PZT 65/35 rod of 0.707-mm radius covered with a spurr coating of 1-mm outer radius. The main difference with respect to the previously shown case of the uncoated rod is that the cutoff frequencies become much lower, partly because of the increased radius and partly because of the lower sound velocity in the coating. In addition, at high frequencies the guided modes drop to a much lower phase velocity than in the uncoated rod, which is also due to the lower sound velocity in the coating.

Figure 6 shows the dispersion curves for the three lowest-order axisymmetric bulk modes in a composite con-

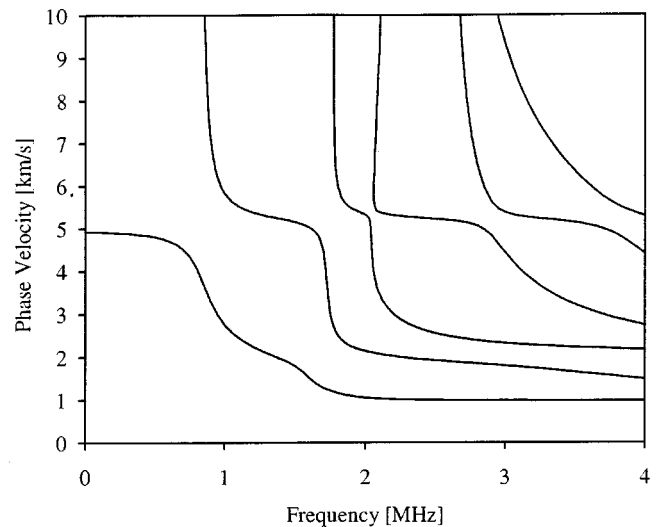


FIG. 5. Dispersion curves for the six lowest-order axisymmetric guided modes in a transversely isotropic piezoelectric PZT 65/35 rod of 0.707-mm radius covered with a spurr coating of 1-mm outer radius.

taining 25% volume fraction of reinforcement. The matrix is isotropic nonpiezoelectric spurr while the periodic reinforcement is made from transversely isotropic piezoelectric PZT 65/35 fibers of 0.707-mm radius.

## V. CONCLUSION

A unified general treatment of elastic guided wave propagation in anisotropic multilayered piezoelectric rod systems was presented. Dispersion relations were derived for either free, immersed, or embedded multilayered rod systems. Individual coaxial layers were assumed to be transversely isotropic and the system global transfer matrix was constructed by applying suitable continuity conditions at the interfaces. By invoking appropriate boundary conditions for multilayered fiber systems having an additional coaxial ma-

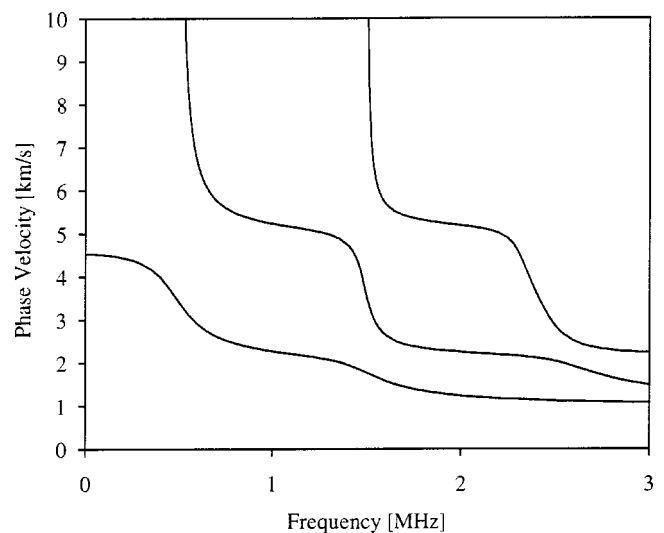


FIG. 6. Dispersion curves for the three lowest-order axisymmetric bulk modes in a composite containing 25% volume fraction of reinforcement. The matrix is isotropic nonpiezoelectric spurr while the periodic reinforcement is made from transversely isotropic piezoelectric PZT 65/35 fibers of 0.707-mm radius.

trix cladding, the same formal solutions were applied to approximate elastic wave propagation along the fibers in infinite composite media containing a periodic distribution of multilayered piezoelectric fiber systems. The analytical results were numerically illustrated through the example of a typical piezoelectric fiber-polymer coating (matrix) arrangement.

- <sup>1</sup>A. H. Nayfeh and P. B. Nagy, "General study of axisymmetric waves in layered anisotropic fibers and their composites," *J. Acoust. Soc. Am.* **99**, 931–941 (1996).
- <sup>2</sup>W. T. Thomson, "Transmission of Elastic Waves Through a Stratified Solid Medium," *J. Appl. Phys.* **21**, 89–93 (1950).
- <sup>3</sup>N. A. Haskell, "Dispersion of Surface Waves on Multilayered Media," *Bull. Seismol. Soc. Am.* **43**, 17–34 (1953).

- <sup>4</sup>A. H. Nayfeh, *Wave Propagation in Layered Anisotropic Media with Applications to Composites* (North-Holland, Amsterdam, 1995).
- <sup>5</sup>H. S. Paul, "Vibration of circular cylindrical shells of piezoelectric silver iodide crystals," *J. Acoust. Soc. Am.* **40**, 1077–1080 (1966).
- <sup>6</sup>V. Winkel, J. E. B. Oliveira, J. D. Dai, and C. K. Jen, "Acoustic Wave Propagation in Piezoelectric Fibers of Hexagonal Crystal Symmetry," *IEEE Trans. Ultrason. Ferroelectr. Freq. Control* **42**, 949–955 (1995).
- <sup>7</sup>S. Minagawa, "Propagation of Harmonic Waves in a Layered Elasto-Piezoelectric Composite," *Mech. Mater.* **19**, 165–170 (1995).
- <sup>8</sup>J. T. Stewart and Y. K. Yong, "Exact Analyses of the Propagation of Acoustic Waves in Multilayered Anisotropic Piezoelectric Plates," *IEEE Trans. Ultrason. Ferroelectr. Freq. Control* **41**, 375–390 (1994).
- <sup>9</sup>A. H. Nayfeh and H. Chien, "The influence of piezoelectricity on reflected waves from fluid-loaded anisotropic plates," *J. Acoust. Soc. Am.* **91**, 1250–1261 (1992).
- <sup>10</sup>L. Adler, "Matrix Methods Applied to Acoustic Waves in Multilayers," *IEEE Trans. Ultrason. Ferroelectr. Freq. Control* **37**, 485–490 (1990).